

Tapered Microchannel for Multi-particles Passive Separation Based on Hydrodynamic Resistance

Ida Laila Ahmad¹, Mohd. Ridzuan Ahmad*²

¹Department of Electronic Engineering, Faculty of Electrical and Electronic Engineering, Universiti Tun Hussein Onn Malaysia

²Department of Control and Mechatronics Engineering, Faculty of Electrical Engineering, Universiti Teknologi Malaysia

*Corresponding author, e-mail: mdrizuan@utm.my

Abstract

Researches on separation of multi-particles utilizing microfluidic have been flourishing in recent years with the aid from advancements in microfabrication design and technology. Generally, separation is beneficial for biomedical application especially involving heterogeneous samples. Due to inherent problems of samples isolation, a simple and efficient separation device is required. Here, we present a passive tapered microchannel for multi-particles separation using hydrodynamic principle. Our emphasis is on the effect of hydrodynamic resistance coupled with tapered microchannel design. In the experiment, successful multi-particles samples separation was observed. The results were further analyzed and were in agreement with the proposed concept. This method opens the route toward robust, low-cost and high-throughput, thus it may holds potential to be integrated as one functional module in Micro Total Analysis System (μ TAS).

Keywords: Passive, Separation, Hydrodynamic, Tapered, Multi-particles

Copyright © 2017 Institute of Advanced Engineering and Science. All rights reserved.

1. Introduction

Nowadays, manipulation and separation of multi-particles are important due to growing needs in various applications such as biological analyses, chemical syntheses and mineral processing [1-3]. In addition, separation is crucial in medical diagnostics for cell classification based on its viability, sub-populations and also disease progress monitoring [4-5], [7]. Traditional separation techniques widely available known as centrifugation and membrane filtration have been used for decades shows limitation in terms of slower time to result, fabrication complexity and requires skilful handling. Compared with traditional separation methods, microfluidic devices have small working volume, reduced costs, less invasiveness and faster analysis time.

Technological advancements in micromachining enabled rapid development of system miniaturization especially microfluidics based research to prosper [6]. A typical Lab-on-Chip (LOC) device includes multiple functional modules: sample transportation and preparation module, separation module, detection and analysis module. As the name suggest, separation module is responsible to isolate, enrich and prepare the samples. Separation or sorting technology can be grouped according to the working principles. Generally, there are three major group namely passive, active and combined separation techniques. Passive techniques do not require external fields, is the simplest method for separation. Common designs include manipulation of flow field, interaction between particles and fabrication of channel structure inside microchannel. These separation techniques are preferred in applications where energy input is of critical concern, offer simple design and straightforward operation. The technique known as Pinched Flow Fractionation (PFF) have been used to separate particles of different sizes [8]. While the effect of inertia and dean flow fractionation were used for cancer cell screening [9, 10], label free cell enrichment [11], classification of cancer stages [12] and various sizes particles separation using dean flow demonstrated by [13, 14]. Moreover, shows example of how Micro Vortex Manipulation via herringbone grooves can be used to separate light and denser particles [15]. Deterministic Lateral Displacement (DLD) technique has successfully

separate cells of different sizes and deformability was demonstrated by [16, 17]. Lastly, the usage of Hydrodynamic Filtration separation was shown by [18, 19].

On the other hand, active separation requires external fields (magnetic, electrical, and optical) to achieve separation. These techniques are superior since they offer better performance, better efficiency and higher throughput however they suffer from bulky apparatus and complex handling. Dielectrophoresis (DEP) is a famous electrical field trapping technique for separation of particles in suspension/medium given by [20-22]. The magnetic separation technique offers several advantages including high specificity, lesser cell damage and shorter sorting time have been used to separate two target cells [23, 24]. Separation using optical field showed the capability to influence cell migration and have been demonstrated by [25,26]. It is known that cell of different intrinsic properties (size, density, and stiffness) travel along different path/trajectory. Lastly, combined techniques referred to device which employs mixture of separation principles in order to attain higher separation throughput.

2. Research Method

2.1. Fluidic Circuit Design

In this work, we developed a microfluidic device with tapered microchannel that can perform passive separation of multi-particles based on hydrodynamic resistance as they pass through the microchannel. The device consists of one inlet, one outlet, and tapered angles of either 6°, 12°, 20° or 25° respectively with height measurement at 10 μ m. The schematic of the proposed microchannel is shown in Figure 1(a)-(b). Table 1 provides the characteristic dimensions of the tapered microchannel and the completed microfluidic size (length x width) is 70mm x 30mm.

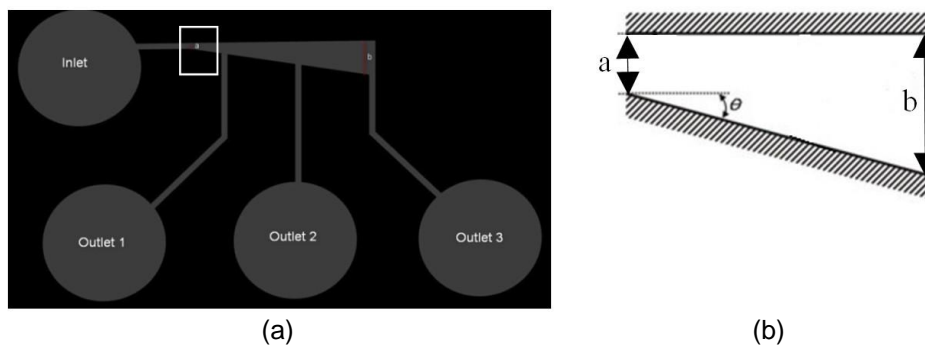


Figure 1. (a) The schematic structure of the proposed microchannel and the inset (b) the taper angle

Table 1. Characteristics Dimensions for Tapered Microchannel

Angle (θ°)	a (μ m)	b (μ m)	a/b	h (μ m)	(a/b):h
6	5	15	0.333	10	0.0333
12	5	25	0.200	10	0.0200
20	5	35	0.143	10	0.0143
25	5	45	0.111	10	0.0111

Figure 2 shows the equivalent electric circuit, where the flow rates in the channels (Q), the pressures (P), and the hydrodynamic resistances (R_h) of the channels, are substituted by electric currents, voltage sources, and electrical resistances respectively. However, this model has its limitation since only purely resistive part is considered to represent steady state behaviour. In order to achieve successful separation, the optimization in terms of R_h value and taper angles were implemented. The optimization was realized using finite element simulation which is elaborated further in the next section. Furthermore, to eliminate any effect of turbulence or microvortex inside the microchannel, the value of Reynolds Number (Re) was always kept in laminar state ($Re < 2000$).

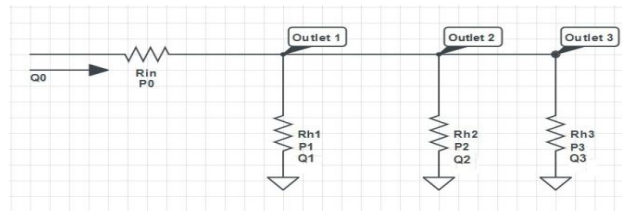


Figure 2. The equivalent resistance circuit

2.2. Working Principles

As the fluid flow inside the microchannel, a mixture containing polydisperse samples was introduced at the inlet. This sample will travel along centreline of the flow profile due to the narrow microchannel (focusing area). As the multi-particles exit the focusing area, they started to travel in different trajectories due to difference of the intrinsic properties such as size, density and deformability. Lateral migration of particles suspended in fluidic environment is influenced by their radius and flow rate. As the tapered microchannel gradually widens out, average velocity at the centre started to become slower. Such that flow near the side outlets is angled downward, creating a streamlines which assists migration of particles towards collection outlets.

The hydrodynamic resistance (R_h) of a particle is defined as resistance induced upon existence of fluid flow inside microchannel. The R_h for tapered geometry can be calculated using formula (1) and R_h for rectangular microchannel is given by (2). Given that η is the fluid's viscosity, L is the length, h is the height, ω_0 and ω_1 are the width ($h \leq \omega$) respectively. C is a constant that depends on the aspect ratio (in this case is equal to 10), P is the perimeter ($2(\omega + h)$), while A is the cross-sectional area of the channel ($\omega \times h$).

$$R_h = \frac{12\eta L}{h^3} \frac{\ln(\frac{\omega_1}{\omega_0})}{\omega_1 - \omega_0} \quad (1)$$

$$R_h = \frac{C\eta L P^2}{A^3} \quad (2)$$

When particles enter the microchannel, more fluid will be diverted to the outlet causing a change in the outlet flow rate (Q). Generally, the value Q is inversely proportional to the R_h . By exploiting this fact, the tapered microchannel design generates flow profiles where the mean flow velocity becomes smaller due to widening of channel geometry and generates different R_h at the respected outlet. Following hydrodynamic trapping concept, successful trapping will take place whenever lower R_h is detected at the outlet. Therefore, one can predict the particle final destination (outlet) provided the R_h value is known. Figure 3 below illustrates how multi-particles can be separated using this concept.

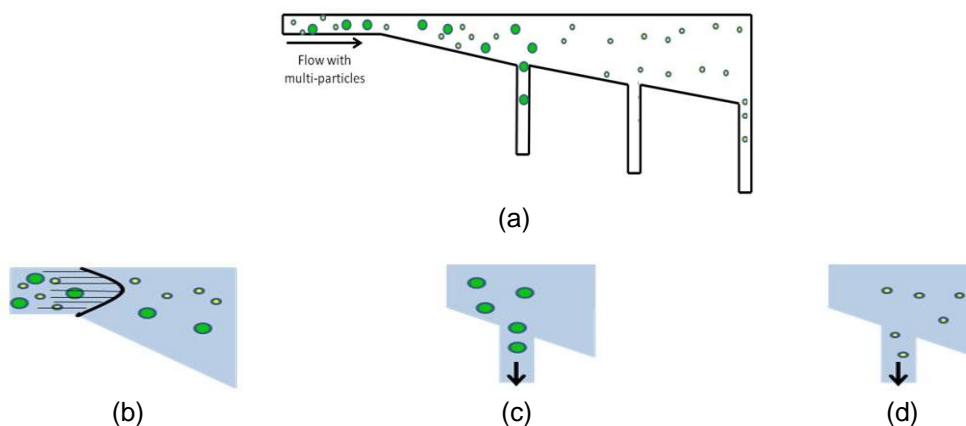


Figure 3. Illustration of separation inside tapered microchannel with multi-particles samples (Yellow and Green) (a) Overall microchannel (b) Flow profile streamlines at the focusing region (c) Trapping of Green particles (d) Trapping of Yellow particle.

In summary, the proposed tapered microchannel conduct the separation mechanism continuously on passive platform. Principle of hydrodynamic was employed thus the concept of R_h and flow profile were used. Moreover, the taper angle helps to manipulate the particle trajectory to guide for successful trapping at the desired outlet. Simple, straight forward mechanism and reliable are clearly advantages to adopt hydrodynamic multi-particles separation.

2.3. Finite Element Simulation

Finite element analysis (FEA) simulation is a common practice for design and optimization for any microchannel. ABAQUS 6.12 by Dassaults System was used since the software possessed multi physics capability which can perform mechanical, electrical and fluid structure interaction. Using dimensions from Table 1, the tapered microchannel was designed using rigid element and Eulerian element was chosen to represent the fluid. However, for the purpose of reducing complexity, the simulation will only evaluate tapered microchannel with two outlets. Multi-particles sample at the inlet were set with polystyrene microbead and Human Servical Epithelial Carcinoma (HeLa cell), the required parameters such as radius, density and Young Modulus were obtained from [27] and were defined at material assignment. Figure 4 shows the complete simulation set up. The finite element model was simplified to use only two outlets due to minimum trapping role of middle outlet. Observation in terms of velocity profiles and separation pattern was carried out.

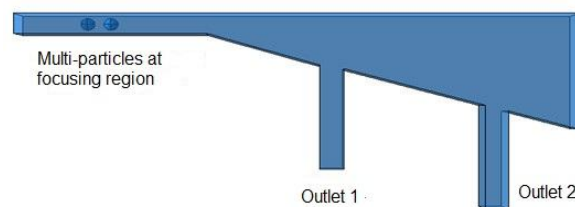


Figure 4. ABAQUS 6.12 simulation set up of tapered microchannel with multi-particles

2.4. Fabrication and Testing

The tapered microchannel used in this study has been fabricated using soft lithography procedures. Briefly, a 2.5 inch glass chrome mask coated with AZP 1350, a positive photoresist was used in order to transfer the microchannel design and printed by a micro pattern generator (μ PG, Heidelberg Instruments, Germany). Next, the unwanted photoresist layer on the mask was removed during development stage. SU8-3005 negative photoresist (Kayaku Microchem, Japan) was used to spin coat on the wafers to obtain the desired thickness. Later, the SU8-coated silicon wafers were soft baked (95°C for 10 minutes). The photoresists film then exposed to the ultraviolet (UV) light using the mask aligner ($200\text{ mJ}/\text{cm}^2$ at 11.8 s) and hardened by two stages post-baked processes (65°C for 1 minute, 95°C for 3 minutes).

Etchant was used to etch away the unexposed SU-8 layer and further developed using Isopropanol (IPA) leaving a positive relief containing microchannel pattern. Surface profiler was used to verify the mold height/thickness obtained. Next, liquid polymethylsiloxane (PDMS) and curing agent (SILPOT 184, SILPOT CAT Dow Corning, USA) were mixed using 9:1 ratio and was poured over the mold. By using convection oven at 65°C , the PDMS was allowed for complete cross-linking in 2 hours. The cured PDMS was peeled from the mold leaving the negative cast of the microchannel pattern. An enclosed PDMS channel was achieved by bonding the PDMS channel with glass slide through plasma oxidation treatment (20 mA, 3 minutes).

In this study, proof of concept was demonstrated using sample comprised of mixture of microbeads and biological cells. Non fluorescent polystyrene microbeads with an average diameter of $10\ \mu\text{m}$ ($\rho=2.0\ \text{g}/\text{cm}^3$; Polysciences Inc., PA, USA). The concentrations of these particles were 5×10^5 per $1\ \mu\text{l}$ respectively. The HeLa cells were cultured in a humidified incubator at 37°C with 5% CO_2 . The culture medium consisted of 90% minimum essential Eagle medium (Sigma-Aldrich) with Eagle's BSS, 2 mM l-glutamine, 1.5 g/l sodium bicarbonate, 0.1

mM non-essential amino acids and 1.0 mM sodium pyruvate+10% fetal bovine serum. The sample was prepared prior to the experiment and suspended in the suspension of culture medium.

Microfluidic device inlet was connected to Legato 180 Syringe Pump (KD Scientific Corp., USA) equipped with 3 ml disposable syringe (Terumo Medical Group). Slow flow rate of (0.5 μ l/min and 1.0 μ l/min) were used. The device operation starts with filling the device with culture medium to remove bubbles or any impurities. Next, the sample was introduced to the inlet. All observations were monitored real-time using inverted microscope IX-71 (Olympus, Japan) with 40x magnification.

3. Results and Analysis

3.1. Simulation of Flow Profiles in Tapered Microchannel

Taper design proved to be useful to reduce the clogging problem due to the widening effect. The velocity of travelling particle is related to fluid flow and can be manipulated from cross sectional area of the tapered microchannel. In terms of velocity the flow stream will be laminar in narrow microchannel but slowly decelerates towards the downstream due to the widening effect. The flow rate in the outlet had to be lower than that in the focusing channel, in order to drive the incoming particles into the widening channel. When this happens, particles of different properties which travel along their own centerline will be further deviated. Figure 5 (a)-(b) illustrate the velocity streamlines for smaller taper angles used (6° and 12°) While Figure 6 (a)-(b) show the streamlines for larger taper angles (20° and 25°). It can be seen that the flow deviation is greater for higher taper angles.

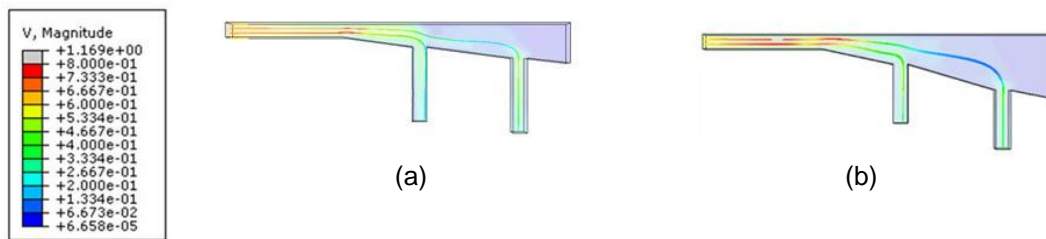


Figure 5. Flow velocity streamlines for (a) Taper angle 6° (b) Taper angle 12°

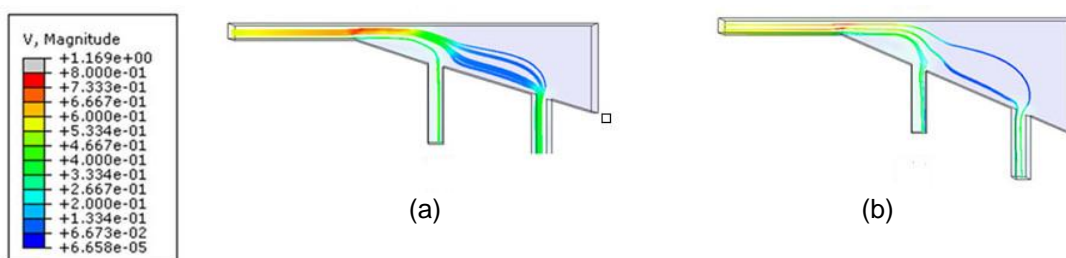


Figure 6. Flow velocity streamlines (a) Taper angle 20° (b) Taper angle 25°

3.2. Resultant Outlet Hydrodynamic Resistance

The hydrodynamic resistance values generated at the outlets were calculated using the formula mentioned in section 2.2 and tabulated in Table 2 below. It can be seen that outlet 2 will always produce lower R_h as compared to outlet 1 due to differences in geometry. This value is very significant while discussing hydrodynamic effect. According to the hydrodynamic principle, successful particle trapping will always occur at the outlet with lower R_h value.

Table 2. Hydrodynamic resistance at the outlets in tapered microchannel

Angle (θ°)	Outlet 1 R_h	Outlet 2 R_h
6	2.42489×10^{-4}	2.28590×10^{-4}
12	1.93521×10^{-4}	1.73819×10^{-4}
20	2.28686×10^{-4}	2.09759×10^{-4}
25	2.01667×10^{-4}	1.82926×10^{-4}

3.3. Simulation of Hydrodynamic Multi-Particles Separation

Simulation set up was similar to Figure 4. The separation pattern for multi-particles was observed and tabulated in Table 3. Unsuccessful separation was observed for taper angles 6° and 12° . Although the streamlines analysis in section 3.1 shows hydrodynamic effect is also experienced by the smaller taper angles, a rather confined geometry does not amplify the particles lateral migration path. On the contrary, successful separation was observed for higher taper angle at 20° and 25° . The particles were able to migrate along their centreline and facilitate separation. However, separation of particles with similar properties proved to follow hydrodynamic principle regardless of the taper angle used.

Table 3. Simulation of multi-particles hydrodynamic separation with different taper angles

Angle (θ°)	Cells only	Microbeads only	Mixture of Cell & Microbeads
6	Outlet 2	Outlet 2	Unsuccessful
12	Outlet 2	Outlet 2	Unsuccessful
20	Outlet 2	Outlet 2	Cell to Outlet 1 Microbead to Outlet 2
25	Outlet 2	Outlet 2	Cell to Outlet 1 Microbead to Outlet 2

3.4. Multi-particles Separation in Tapered Microchannel

Particles that were initially positioned near to or along the wall of the inlet reservoir eventually distributed to collection Outlet 1 and these particles tend to have the largest diameter (HeLa cell). Next, microbeads collected at furthest outlet (outlet 3) normally have the smallest diameter. It is expected that, particles with an intermediate diameter will be collected at the middle outlet in the real experiment (with three outlets). This predicted performance suggests that passive sorting of particles could be realized, using only hydrodynamic resistance of the outlets enable successful separation. In addition, the effect of taper angles created unique streamlines which controlling the migration path of particles without external perturbation. Therefore, microchannel design amplifies the effect further for faster and better particle enrichment at outlet. Figure 7 (a)-(c) illustrates the separation process and results in tapered microchannel.

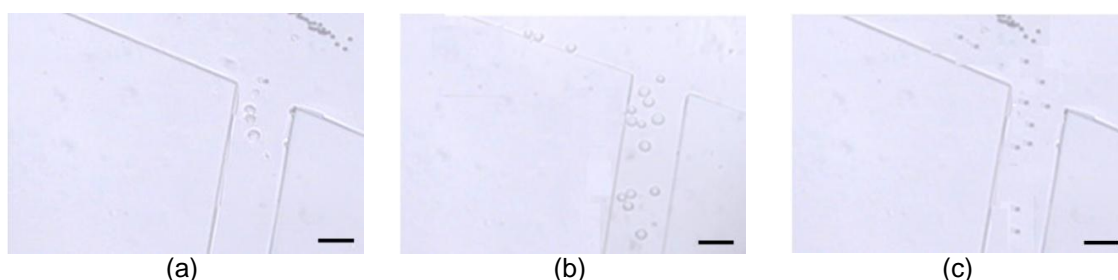


Figure 7. (a) Successful separation between HeLa cells and microbeads (b) HeLa cells collected at outlet 1 (c) Microbeads collected at outlet 3. Size bar is $10\mu\text{m}$

Considering the effect of hydrodynamic and differential velocity produced at bifurcation of three side outlets created flow imbalance causing the bigger particles (HeLa cells) to be directed to outlet 1. Moreover, increasing width due to tapered design facilitate migration of

smaller radius particles (microbeads) towards the furthest outlet. Figure 8 below show the size distribution measurement and purity of samples collected at the outlets.

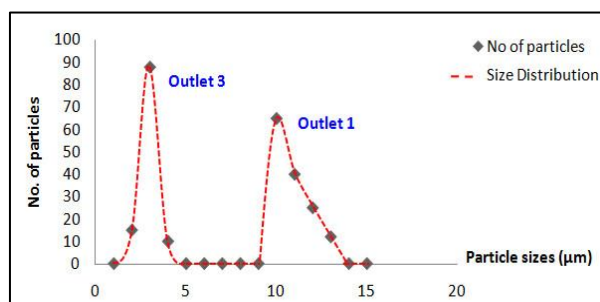


Figure 8. Size distribution measurement at the outlet with ~100% purity of samples collected.

4. Conclusion

A concept of hydrodynamic separation using tapered microchannel has been proposed, and the validity of this method was successfully demonstrated. The results showed that the design is suitable for the separation of polydisperse multi-particles since the simple introduction of samples suspension enables accurate and relatively fast separation. It is expected that the presented microfluidic systems can be used for various applications. By optimizing the operating conditions and manipulating other parameters such as sample concentration and flow rate, the throughput will be greatly improved using the same devices.

References

- [1] Manz A, Harrison DJ, Verpoorte EM, Fettinger JC, Paulus A, Lüdi H, Widmer HM. Planar chips technology for miniaturization and integration of separation techniques into monitoring systems: capillary electrophoresis on a chip. *Journal of Chromatography A*. 1992; 593(1): 253-258.
- [2] Reyes DR, Iossifidis D, Auroux PA, Manz A. Micro total analysis systems. 1. Introduction, theory, and technology. *Analytical chemistry*. 2002; 74(12): 2623-2636.
- [3] Sajeesh P, Sen AK. Particle separation and sorting in microfluidic devices: a review. *Microfluidics and nanofluidics*. 2014; 17(1): 1-52.
- [4] Suresh S, Spatz J, Mills JP, Micoulet A, Dao M, Lim CT, Beil M, Seufferlein T. Connections between single-cell biomechanics and human disease states: gastrointestinal cancer and malaria. *Acta biomaterialia*. 2005; 1(1): 15-30.
- [5] Alshareef M, Metrakos N, Perez EJ, Azer F, Yang F, Yang X, Wang G. Separation of tumor cells with dielectrophoresis-based microfluidic chip. *Biomicrofluidics*. 2013; 7(1): 011803.
- [6] Whitesides GM. The origins and the future of microfluidics. *Nature*. 2006 Jul 27;442(7101):368-373.
- [7] Vaziri A, Gopinath A. Cell and biomolecular mechanics in silico. *Nature materials*. 2008; 7(1): 15-23.
- [8] Yamada M, Nakashima M, Seki M. Pinched flow fractionation: continuous size separation of particles utilizing a laminar flow profile in a pinched microchannel. *Analytical chemistry*. 2004; 76(18): 5465-5471.
- [9] Rivet C, Lee H, Hirsch A, Hamilton S, Lu H. Microfluidics for medical diagnostics and biosensors. *Chemical Engineering Science*. 2011; 66(7): 1490-1507.
- [10] Dong Y, Skelley AM, Merdek KD, Sprott KM, Jiang C, Pierceall WE, Lin J, Stocum M, Carney WP, Smirnov DA. Microfluidics and circulating tumor cells. *The Journal of Molecular Diagnostics*. 2013; 5(2): 149-157.
- [11] Hur SC, Henderson-MacLennan NK, McCabe ER, Di Carlo D. Deformability-based cell classification and enrichment using inertial microfluidics. *Lab on a Chip*. 2011; 11(5): 912-920.
- [12] Lee WC, Bhagat AA, Huang S, Van Vliet KJ, Han J, Lim CT. High-throughput cell cycle synchronization using inertial forces in spiral microchannels. *Lab on a Chip*. 2011; 11(7): 1359-1367.
- [13] Gossett DR, Carlo DD. Particle focusing mechanisms in curving confined flows. *Analytical chemistry*. 2009; 81(20): 8459-8465.
- [14] Bhagat AA, Kuntaegowdanahalli SS, Papautsky I. Continuous particle separation in spiral microchannels using dean flows and differential migration. *Lab on a Chip*. 2008; 8(11): 1906-1914.
- [15] Hsu CH, Di Carlo D, Chen C, Irimia D, Toner M. Microvortex for focusing, guiding and sorting of particles. *Lab on a Chip*. 2008; 8(12): 2128-2134.

- [16] Huang LR, Cox EC, Austin RH, Sturm JC. Continuous particle separation through deterministic lateral displacement. *Science*. 2004; 304(5673): 987-990.
- [17] Beech JP, Tegenfeldt JO. Tuneable separation in elastomeric microfluidics devices. *Lab on a Chip*. 2008; 8(5): 657-659.
- [18] Yamada M, Seki M. Hydrodynamic filtration for on-chip particle concentration and classification utilizing microfluidics. *Lab on a Chip*. 2005; 5(11): 1233-1239.
- [19] Yamada M, Seki M. Microfluidic particle sorter employing flow splitting and recombining. *Analytical chemistry*. 2006; 78(4): 1357-1362.
- [20] Gascoyne PR, Wang XB, Huang Y, Becker FF. Dielectrophoretic separation of cancer cells from blood. *IEEE transactions on industry applications*. 1997; 33(3): 670-678.
- [21] Nascimento EM, Nogueira N, Silva T, Braschler T, Demierre N, Renaud P, Oliva AG. Dielectrophoretic sorting on a microfabricated flow cytometer: label free separation of Babesia bovis infected erythrocytes. *Bioelectrochemistry*. 2008; 73(2): 123-128.
- [22] Holmes D, Morgan H. Cell positioning and sorting using dielectrophoresis. *European Cells and Materials*. 2002; 4(Supple): 120-122.
- [23] Adams JD, Kim U, Soh HT. Multitarget magnetic activated cell sorter. *Proceedings of the National Academy of Sciences*. 2008; 105(47): 18165-18170.
- [24] Kersaudy-Kerhoas M, Dhariwal R, Desmulliez MP, Jouvét L. Hydrodynamic blood plasma separation in microfluidic channels. *Microfluidics and nanofluidics*. 2010; 8(1): 105-114.
- [25] Ladavac K, Kasza K, Grier DG. Sorting mesoscopic objects with periodic potential landscapes: optical fractionation. *Physical Review E*. 2004; 70(1): 010901.
- [26] Glückstad J. Microfluidics: Sorting particles with light. *Nature Materials*. 2004; 3(1): 9-10.
- [27] Kuroda C, Ohki Y, Ashiba H, Fujimaki M, Awazu K, Tanaka T, Makishima M. *Microfluidic sedimentation system for separation of plasma from whole blood*. In IEEE SENSORS 2014 Proceedings. 2014: 1854-1857.